

Character of the smectic-*A* – chiral-smectic-*C* phase transition near a chiral-nematic – smectic-*A* – chiral-smectic-*C* point

J. Zubia

Departamento de Automática, Electrónica y Telecomunicaciones, Escuela Técnica Superior de Ingenieros Industriales y de Telecomunicación, Universidad de País Vasco, Alameda de Urquijo s/n, 48013 Bilbao, Spain

M. Castro and J. A. Puértolas

Departamento de Ciencia y Tecnología de Materiales y Fluidos, Centro Politécnico Superior de Ingenieros, Universidad de Zaragoza, 50015 Zaragoza, Spain

J. Etxebarria

Departamento de Física de la Materia Condensada, Facultad de Ciencias, Universidad del País Vasco, Apartado 644, 48080 Bilbao, Spain

M. A. Pérez Jubindo and M. R. de la Fuente

Departamento de Física Aplicada II, Facultad de Ciencias, Universidad del País Vasco, Apartado 644, 48080 Bilbao, Spain

(Received 8 March 1993)

Binary mixtures of two compounds with phase sequences isotropic (*I*)–chiral-nematic (*N*)–chiral-smectic-*C* (*C*^{*}) and *I*–*N*–smectic-*A* (*A*)–*C*^{*} have been investigated. Spontaneous-polarization and tilt-angle measurements near the *A*–*C*^{*} transition indicate a mean-field-like to tricritical crossover behavior near the *N*–*A*–*C*^{*} point of the phase diagram, the critical exponent β varying continuously from values near 0.5 to almost 0.25. The heat capacity has also been measured with a high-resolution ac calorimetric technique at the *A*–*C*^{*} and *N*–*A* transitions of three mixtures. It is found that the *A*–*C*^{*} transition is well described by an extended mean-field model. The fits show that, in accordance with polarization and tilt-angle measurements, the transition evolves from a second-order regime towards tricriticality as the *A* range decreases. Based on these results and other analogous studies published by other authors, some considerations about the material requirements necessary to obtain first-order *A*–*C*^{*} transitions are briefly discussed.

PACS number(s): 61.30.–v, 64.70.Md, 64.60.Kw

I. INTRODUCTION

The character of the smectic-*A* to smectic-*C* or chiral-smectic-*C* (*A*–*C* or *A*–*C*^{*}) phase transition is a subject of considerable interest. Usually, *A*–*C* (or *C*^{*}) transitions are second order. However, recent observations on ferroelectric compounds with high spontaneous polarization have demonstrated the possibility of existence of first-order *A*–*C*^{*} transitions [1–3].

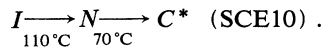
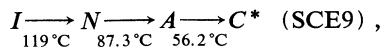
On the other hand, the properties of the nematic (or chiral nematic) – *A*–*C* (*NAC*) point have received great attention. One important question about the *NAC* point is the location of the tricritical point on the *A*–*C* line. Experimental works performed on binary systems obtained by mixing materials with sequences *N*–*C* and *N*–*A*–*C* have shown that the tricritical point is very near the *NAC* point [4–7]. However, in view of the existence of first-order *A*–*C*^{*} transitions, there exists the possibility of obtaining a tricritical point displaced from the *NAC*^{*} point. Given our current understanding on the mechanisms driving the *A*–*C*^{*} transition to first-order character, a tricritical point away from the *NAC*^{*} composition would be likely to appear in a mixture with a rather narrow *A* range [3,8] and/or with a high spontaneous polar-

ization at the *C*^{*} phase [3,9,10] or at least with large molecular dipole moments [11].

In this paper we report on a study of the *A*–*C*^{*} transition carried out on binary mixtures prepared from two compounds with a first-order sequence *N*–*C*^{*} and a second-order sequence *N*–*A*–*C*^{*}. Both compounds present a medium value of the spontaneous polarization (≈ 20 nC/cm^{–2}) and a broad range of *N* phase. The nature of the *A*–*C*^{*} line has been analyzed by means of spontaneous polarization and tilt-angle measurements. The results show a mean-field-like to tricritical crossover behavior as the *NAC*^{*} point is approached. X-ray measurements for mixtures near the *NAC*^{*} composition confirm the continuous character of the *A*–*C*^{*} transition along the entire *A*–*C*^{*} line. Likewise, high-resolution ac calorimetric measurements support the above idea and the specific-heat anomalies associated to the *A*–*C*^{*} transitions are well described by the usual extended Landau free energy. Finally, based on these results and analogous studies reported in the literature, some considerations about the materials requirements necessary to obtain first-order *A*–*C* transitions are discussed. In this sense, the importance of a narrow (or inexistent) *N* phase is particularly stressed.

II. EXPERIMENT

The materials studied are binary mixture of two compounds SCE9 and SCE10, which were purchased from BDH, London. Both materials are multicomponent mixtures with a large cholesteric pitch over a broad temperature range above the smectic mesophases. The phase sequences as determined by texture observation are the following:



Here *I* stands for the isotropic phase. Ten different mixtures were studied, with SCE9 concentrations $x=1, 0.74, 0.48, 0.22, 0.18, 0.15, 0.13, 0.07,$ and 0 (weight fraction).

Tilt angle and spontaneous polarization were measured on sample cells with an area of $4 \times 4 \text{ mm}^2$ and a thickness of $4 \mu\text{m}$. The glass plates were treated with nylon 6/6 and rubbed unidirectionally in order to achieve the desired bookshelf geometry [12]. The materials were introduced into the cells by capillary action in the *I* phase and cooled slowly ($0.1^\circ\text{C min}^{-1}$) down to the ferroelectric phase. Previously to the experiments, all samples were rigorously examined to check the alignment quality.

The tilt angle was determined optically by measuring the switching angle between the director positions at positive and negative applied electric fields [13]. The spontaneous polarization was measured using the triangular-wave method [14,15]. The experiments were performed dynamically at a constant rate of $0.1^\circ\text{C min}^{-1}$ both on heating and cooling.

X-ray measurements were conducted using an automatic powder diffractometer (STOE). For these measurements, capillaries of diameter 0.5 mm filled with unaligned samples were used. The temperature of the sample was controlled with a homemade oven with a temperature stability of 0.1°C . Copper $K\alpha_1$ and $K\alpha_2$ lines were separated and only the former was used for the experiments. The accuracy in the determination of the Bragg angle was 0.001° .

Specific-heat measurements were performed using a high-resolution ac calorimeter whose essential features are based on a previous one described in the literature [16]. Some modifications were introduced in order to improve its versatility and resolution. The details of the calorimeter have been described elsewhere [17]. Here we will briefly review its basic characteristics.

The source of the modulated input power is a strain gauge which operate as a resistive heater and as the support of the sample holder. The sensor for detecting the temperature oscillations is a microbead thermistor supplied by a high-stability home-built dc current generator. A lock-in amplifier (EG&G PARC 5302) acts as oscillator for the heater and also measures the ac voltage and phase shift generated in the thermistor. The sample holder is a commercial aluminum capsule used for differential-scanning-calorimetry (DSC) measurements, with a volume of $10 \mu\text{l}$ and a diameter of 10 mm. It has the advantage of facilitating sample preparation and permits to compare the data with preliminary DSC measure-

ments performed on the same sample. The sample holder is surrounded by two concentric copper blocks where vacuum can be made or helium can be introduced in order to control the thermal link of the cell. The whole system is immersed into a thermostatic bath (Lauda KP20) and the temperature controller allows to scan the temperature with different rates from 100 to 5000 mK h^{-1} . The external block reduces the influence of thermal fluctuations of the bath on the temperature of the cell. As a result, temperature oscillations in the sample are less than 1 mK during long time when the bath is in thermal equilibrium. The temperature of the block is monitored by a platinum resistance and measured by a multimeter (Hewlett Packard 3457 A). Finally, all the equipment is interfaced to a personal computer through Institute of Electrical and Electronics Engineers circuit boards. The resolution of the calorimeter is estimated to be better than 0.1%.

III. RESULTS AND DISCUSSION

A. Polarization and tilt

Figures 1 and 2 show the temperature dependence of the spontaneous polarization P_s and tilt angle θ of the compounds SCE9 and SCE10, respectively. As expected, the material SCE9 presents a gradually changing polarization and tilt, starting from zero at the *A*-*C** transition and continuously increasing as temperature goes down. On the other hand, the discontinuous character of the *N*-*C** transition is clearly visible in the polarization and tilt behavior of SCE10, where jumps about 8 nC cm^{-2} in the polarization and 15° in the tilt are observed at the transition point.

Binary mixtures prepared from SCE9 and SCE10 present the phase diagram represented in Fig. 3. The transition temperatures were determined on freshly prepared samples from measurements of the electroclinic effect at the *N* and *A* phases and direct microscopic observation. As can be seen, as the SCE9 concentration decreases the *A* range becomes smaller. The *NAC** point is attained for a SCE9 concentration $x_c = 0.12 \pm 0.01$.

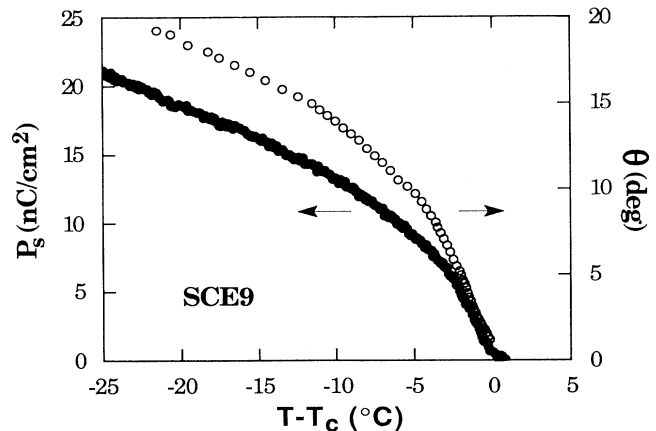


FIG. 1. Temperature dependence of the spontaneous polarization and tilt angle in the *C** phase of compound SCE9.

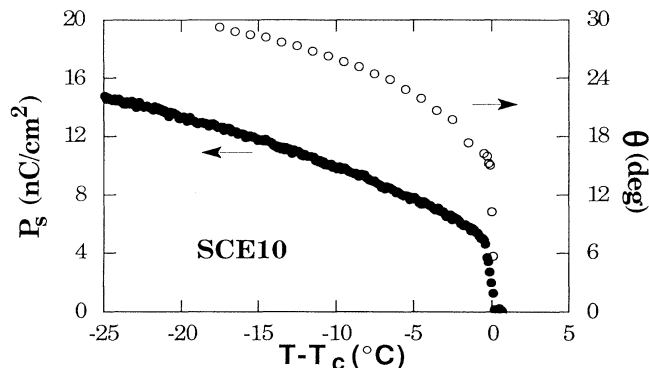


FIG. 2. Temperature dependence of the spontaneous polarization and tilt angle in the C^* phase of compound SCE10. The first-order character of the $N-C^*$ transition is clearly visible.

We will only present some of the results obtained on various mixtures with $x > x_c$. For $x < x_c$, clear jumps in P_s and θ similar to those in Fig. 2 confirmed unambiguously the well-known first-order character of the $N-C^*$ transition. Figures 4(a) and 4(b) show the polarization and tilt data of several materials with $x \geq x_c$. The variations of P_s and θ near the $A-C^*$ transition are steeper as the concentration x_c is approached. However, no signs of discontinuity appear, which suggests a second-order character for the transition along the entire $A-C^*$ line. In order to confirm this point we analyzed the data using a simple power law

$$\theta = \theta_0(T_c - T)^\beta, \quad P_s = P_0(T_c - T)^{\beta'} \quad (1)$$

where T_c is the $A-C^*$ transition temperature and θ_0 and P_0 are constants.

It should be noted that the former expressions must not perfectly hold (in a reasonable temperature range) if the data are expected to be well described by a mean-field model with a small fourth-order term and an important sixth-order term, as usually happens in these materials.

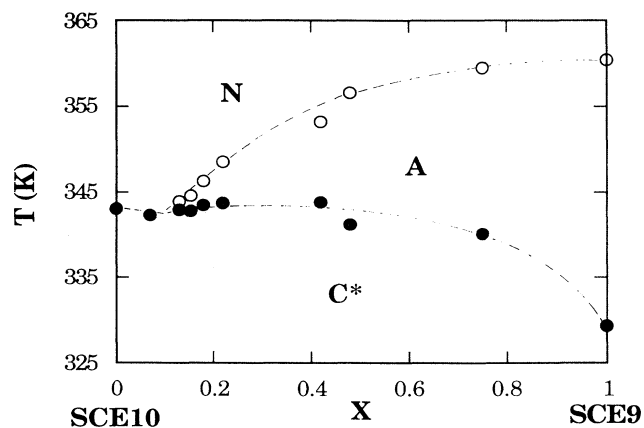


FIG. 3. Phase diagram for SCE9+SCE10 liquid-crystal mixtures; x is the weight fraction of SCE9. Dashed lines have been drawn only for eye-guiding purposes.

In this sense, β and β' should be considered as “effective” critical exponents whose values depend on the fitting range and are well defined only in the limit cases of ordinary mean-field behavior ($\beta, \beta' = 0.5$) and a tricritical point ($\beta, \beta' = 0.25$). In fact, in all the samples studied the β and β' values obtained in the fits were always between these two limiting values, signifying a behavior intermediate between mean field and tricritical. On the other hand, it was found that β and β' decreased with increasing fitting range so, in order to compare among the different samples, the range was arbitrarily fixed to 5°C in all cases. Figure 5 represents the evolution of the exponents calculated in this way. As can be seen, β and β' are quite similar, indicating that P_s and θ are approximately proportional to each other. Furthermore, a clear tendency is observed from exponent values near 0.5 towards values close to 0.25 as the A range shrinks. In addition, it was found that mixtures with the largest and smallest A ranges could be fitted successfully to the above power laws in larger temperature intervals without

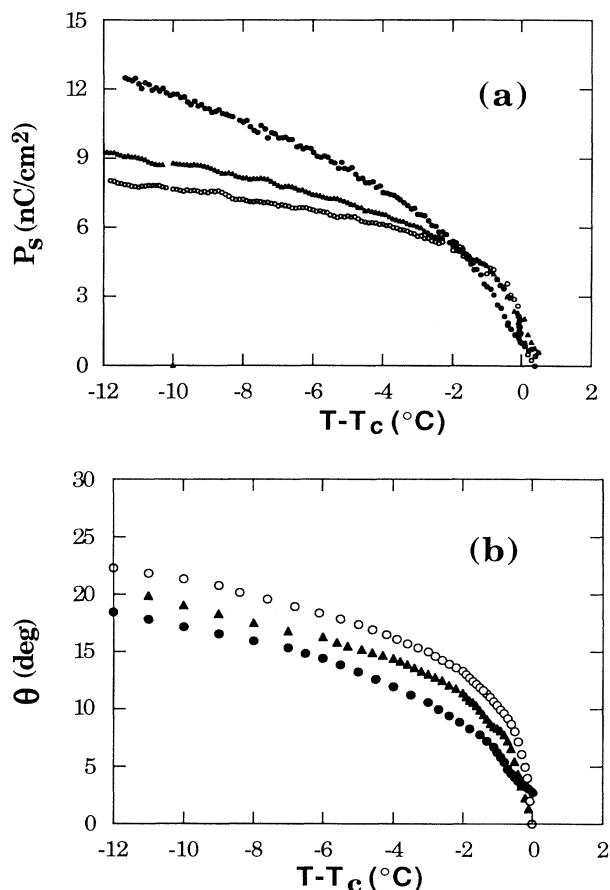


FIG. 4. Temperature dependence of the (a) spontaneous polarization and (b) tilt angle for several SCE9+SCE10 mixtures. Open circles, triangles, and solid circles represent mixtures with concentrations $x = 0.13, 0.15$, and 0.48 , respectively. The variation of both polarization and tilt near T_c are steeper as the composition approaches $x_c = 0.12$, which corresponds to the NAC^* point.

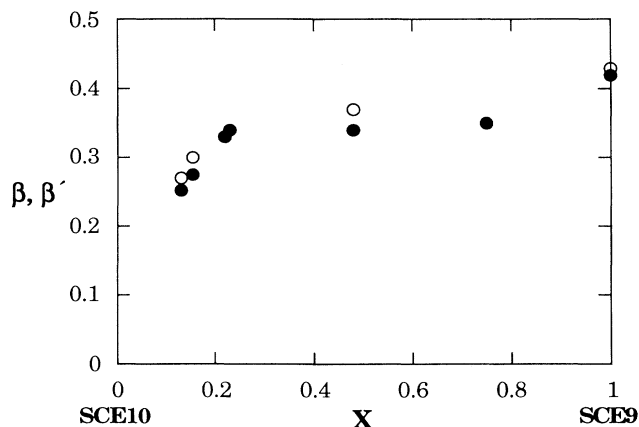


FIG. 5. Evolution of the critical exponents for the spontaneous polarization β' (solid circles) and tilt β (open circles) as a function of the SCE9 concentration. Both β and β' are increasing functions of x , starting from a close to tricritical value (0.27) near x_c .

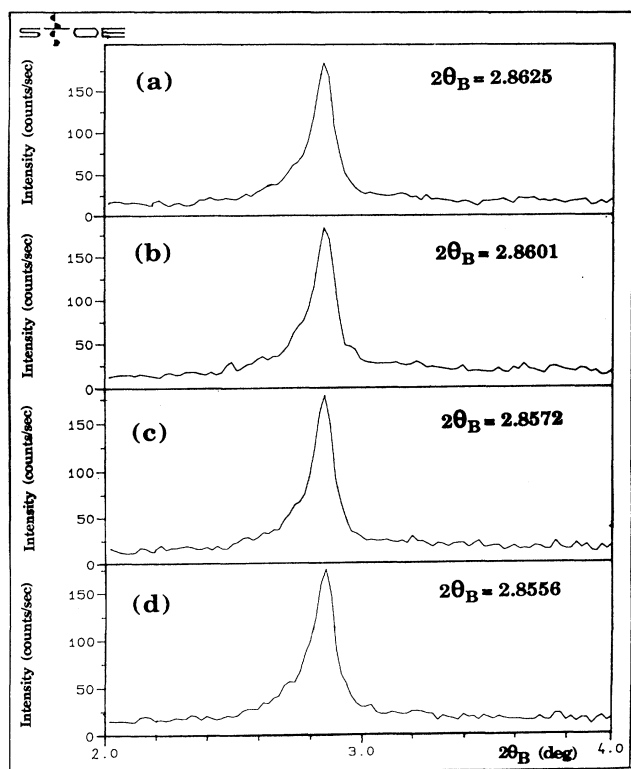


FIG. 6. Raw diffractometer traces obtained along the equatorial direction around the $A-C^*$ transition for the mixture with $x=0.13$. (a) $T-T_c=0.1^\circ\text{C}$, (b) $T-T_c=-0.1^\circ\text{C}$, (c) $T-T_c=-0.2^\circ\text{C}$, and (d) $T-T_c=-0.3^\circ\text{C}$. No coexistence of two density modulations can be appreciated and the Bragg angle corresponding to the peak maximum (θ_B) presents a continuous evolution.

important variations of the exponents. All these factors indicate clearly a mean-field to tricritical crossover behavior along the $A-C^*$ line.

It is, however, difficult to decide the character of the $A-C^*$ transition for x close to x_c only with the above measurements. The spontaneous polarization and tilt angle were measured by applying a strong electric field which can alter the intrinsic values of these quantities and smear out possible (small) discontinuities at the transition point. In order to solve this problem, x-ray measurements were performed on the mixtures with 1 and 2°C of A range ($x=0.13$ and 0.15). The results can be summarized as follows. No coexistence of the diffraction peaks corresponding to the density modulations of the A and C^* phases was found (see Fig. 6). Moreover, the Bragg angle presented a continuous evolution and no jump was observed around the phase transition. Thus we are induced to think that the $A-C^*$ transition is always second order. Therefore, the tricritical point on the $A-C^*$ line must be in the vicinity or at the NAC^* point.

B. Heat capacity

Three samples, with weight fractions of SCE9 $x=0.48$, 0.22, and 0.13, were studied over a wide temperature range spanning the $N-A$ and $A-C^*$ transitions. The sample weight was in all cases about 25 mg. For all the samples the operating frequency was fixed at 30 mHz, around which linearity between the inverse ac signal and frequency was observed. The scan rate through the different transitions was about 600 mK h^{-1} and the temperature oscillations in the sample were about 60 mK for an input power of 2.5 mW and a helium pressure in the internal chamber of 8 kPa.

Small drifts in the transition temperatures were observed in successive heating and cooling runs. However, the overall shape and size of the excess heat capacity associated to the transitions remained essentially unaltered. We report here the data obtained during the first cooling runs.

Apart from the mentioned drifts, no thermal hysteresis could be detected in any of the transitions. This fact, together with the lack of any noticeable phase shift of the lock-in signal during the measuring process ($<0.01^\circ$), suggests a second-order character for all the transitions.

The overall variation in the total specific heat (sample plus addenda) through both the $N-A$ and $A-C^*$ transitions is shown in Fig. 7 for the $x=0.48$ sample. The anomalies corresponding to the transitions are clearly visible. The increase in C_p at the high temperature region is due to the beginning of the anomaly associated to the $I-N$ transition.

In order to analyze the data, the excess heat capacity ΔC_p must be obtained and, therefore, appropriate background curves have to be estimated. This task is not trivial in our case since the $I-N$, $N-A$, and $A-C^*$ transitions are rather close to each other. For calculating the excess heat capacity associated to the $A-C^*$ transition we chose as base line the extrapolation at low temperatures of the polynomial fit of the total specific heat in the region above the $A-C^*$ transition and below the $N-A$ tran-

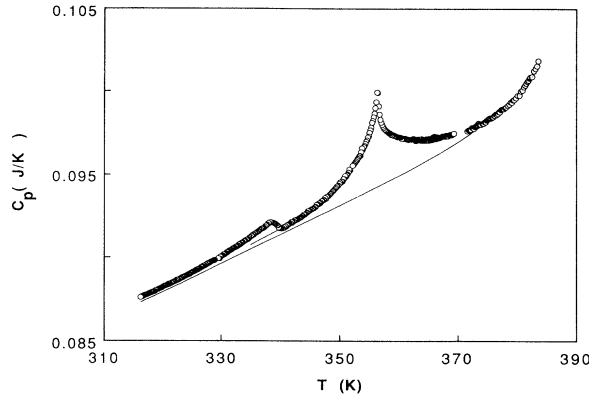


FIG. 7. Experimental heat capacity for the SCE9+SCE10 mixture with $x=0.48$ (48 wt. % of SCE9). Continuous curves represent the baselines used to obtain the excess heat capacity associated to the $A-C^*$ and $N-A$ transitions.

sition. In the case of the $N-A$ transition a similar extrapolation of the points of the “tail” associated with the $I-N$ anomaly was carried out. The resulting background curves are shown by continuous lines in Fig. 7 for the $x=0.48$ mixture. The ΔC_p data corresponding to the $A-C^*$ and $N-A$ transitions are represented in Figs. 8 and 9, respectively, as a function of their corresponding reduced temperatures $t = (T - T_c)/T_c$. There is no curve in Fig. 9 for the $x=0.13$ mixture because, within the experimental resolution, no C_p anomaly could be detected for the $N-A$ transition of this sample.

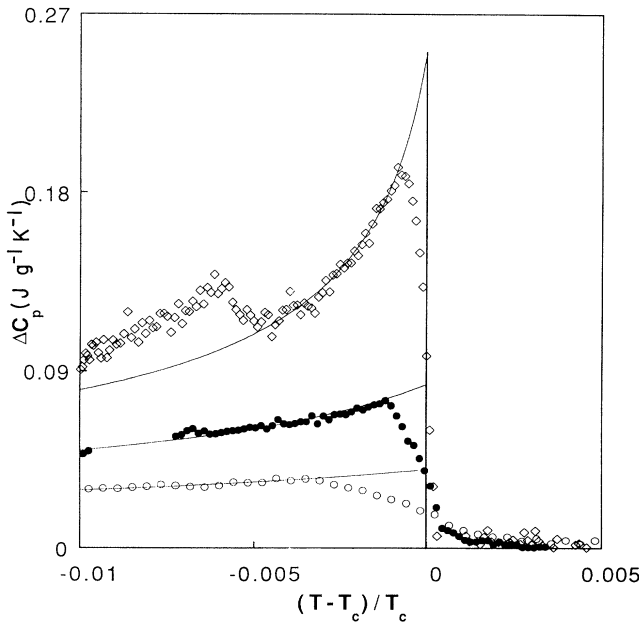


FIG. 8. Excess heat capacity ΔC_p due to the $A-C^*$ transition as a function of the reduced temperature for mixtures with $x=0.48$ (open circles), 0.22 (solid circles), and 0.13 (rhombs). Solid lines are fits to the theoretical predictions of the Landau model.

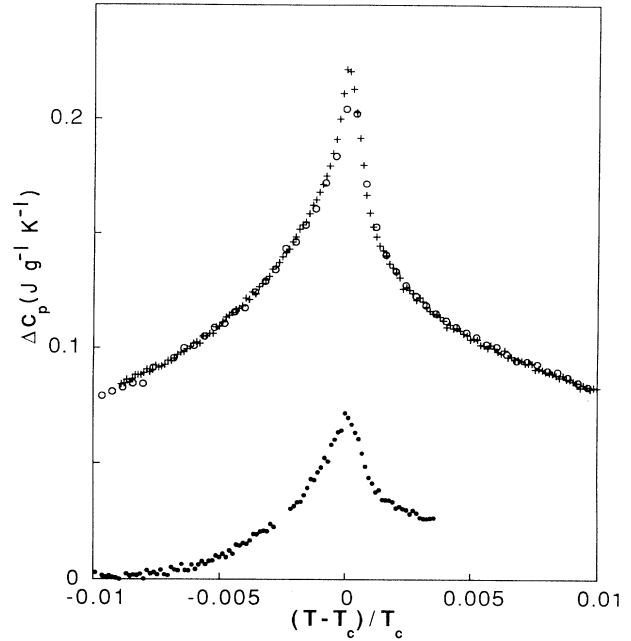


FIG. 9. Excess heat capacity ΔC_p associated to the $N-A$ transition as a function of the reduced temperature for mixtures with $x=0.48$ (open circles) and 0.22 (solid circles). Measurements were obtained on cooling. For comparison, the results on heating for the $x=0.48$ sample are also included (crosses). The lack of thermal hysteresis is clearly visible.

The $A-C^*$ transitions were analyzed using the so-called extended Landau model. According to this approach the free energy of the smectic- C^* phase relative to that of the smectic- A phase is given by

$$G = a\theta^2 + b\theta^4 + c\theta^6 \quad (2)$$

where a and c are positive constants and the sign of b determines the transition character. If $b > 0$, the transition is second order while it is first order for $b < 0$. The value $b = 0$ corresponds to the tricritical point. From the above free-energy expansion, the temperature dependence of the excess heat capacity is obtained as

$$\Delta C_p(T) = T \frac{A}{T_c^2} \left[\frac{T_m - T}{T_c} \right]^{-1/2} \quad (3)$$

where $A = (a^3/12c)^{1/2}$ and $T_m = T_c(1 + b^2/3ac)$. If $b > 0$ the theoretical ΔC_p drops to zero above T_c and Eq. (3) is only valid for temperatures $T < T_c$. In a first-order case, the transition does not take place at T_c but at a higher temperature $T'_c = T_c(1 + b^2/4ac)$ and the ΔC_p expression holds up to this temperature value.

In the fit process the parameter T_c was fixed at the temperature at the midpoint of the heat capacity jump. Just above T_c a non-Landau ΔC_p tail can be observed for the three samples which increases as the A range becomes smaller. This fact suggests that the excess ΔC_p above T_c can be associated to pretransitional fluctuations, although perhaps sample impurities or inhomogeneities

TABLE I. Least-squares values of the fitting parameters appearing in Eq. (3) for the excess heat capacity associated to the *A*-*C** transitions.

Mixture <i>X</i>	T_c (K)	T_m (K)	A (J g^{-1})	ΔC_p Theor. (T_c) ($\text{J g}^{-1} \text{K}^{-1}$)
0.48	339.42	343.48	1.513	0.0407
0.22	345.28	347.27	2.182	0.0833
0.13	345.37	345.77	2.955	0.2514

can also produce the same effect [18]. Continuous lines in Fig. 8 show the Landau fits for the three samples studied and the resulting parameters are given in Table I. These parameters were obtained by means of a linear fit of $(T/\Delta C_p)^2$ vs temperature. It was found that the temperature range in which the linear relationship between these quantities is satisfied depends somewhat on the choised background. However, the values of the slopes and intercepts of the straight lines remained much less affected.

As can be seen, with the exception of a small region around the transition, the fits are rather good for the $x=0.48$ and 0.22 samples. Keeping aside for the moment the anomalous ΔC_p hump detected for the $x=0.13$ mixture, a clear tendency for the behavior of the b parameter can be deduced from the data of Table I. This is evident if the evolution of the theoretical ΔC_p at T_c (given by $a^2/2bT_c$) or the difference between T_m and T_c (equal to $b^2T_c/3ac$) are examined. From both sets of data the conclusion is reached that b tends to zero as the *NAC** point is approached, remaining positive along the whole *A*-*C** line.

It is interesting to examine closer the anomalous behavior of the $x=0.13$ sample. First of all, and as has been pointed out before, there is no evidence of the presence of the *N*-*A* transition. This is not unusual and reflects the fact that the correlation lengths for *A* fluctuations at the *N* phase grow rapidly as the *A* range vanishes, leading to very small C_p anomalies [19]. What is unexpected is the complex structure of the *A*-*C** peak, with an additional small but reproducible shoulder approximately 2°C below the jump. We do not know at present the origin of this effect. As has been shown before, neither the spontaneous polarization nor the tilt angle presented any anomaly in this region. The most likely hypothesis is in our opinion that some composition inhomogeneities or chemical degradation may have occurred in this sample that could have affected our results. This is supported by the relatively high chemical instability [20] of one of the mixture components (SCE10) in which this sample is rich and the long time elapsed between polarization and tilt-angle studies and calorimetric investigations (more than six months). We plan to prepare new mixtures and investigate this point more thoroughly in the near future.

We will finish this section with a brief mention of the *N*-*A* transitions for the sake of completeness. For the two samples analyzed ($x=0.48$ and 0.22), good fits were obtained using the renormalization-group expression including first-order corrections-to-scaling terms, i.e.,

$$\Delta C_p = A^\pm |t|^{-\alpha} (1 + D^\pm |t|^{0.5}) + B \quad (4)$$

where the plus and minus signs refer to above or below the transition point and A , B , D , and α are constants. Fits allowing the critical exponent to vary gave α values close to zero, compatible with the well-known theoretical prediction $\alpha = -0.007$ of the three-dimensional *XY* model. This is in agreement with the expectations [21], given the small McMillan ratios (0.90 and 0.92) of both samples.

C. Character of the *A*-*C** transition

From the above measurements we have concluded that the tricritical point on the *A*-*C** line is at or near the *NAC** point. This is not surprising since analogous results have been observed in other binary systems composed by chiral as well as nonchiral molecules. In fact, except for a few examples recently reported, the *A*-*C* (or *C**) transition has been always found to be continuous. However, it is interesting to comment on the reason for this behavior and discuss the possible circumstances that can drive the transition to be first order.

Up to now several possible factors determining the order of this transition have been pointed out in the literature. For example, it has been found systematically that a narrowing of the *A* temperature range can give rise to first-order *A*-*C** transitions [5,8,22]. The spontaneous polarization magnitude at the *C** phase is also believed to have some influence in this respect [3,9]. Finally the size of the transverse dipole moment of the constituent molecules has been also mentioned as an important factor on the nature of the transition [11]. Some theoretical treatments supporting these ideas have already appeared in the literature, but the relative importance of these factors is still uncertain. Here we will just point out another factor which can promote discontinuity in the *A*-*C* transition and, as far as we know, has not been mentioned in previous works. In compiling our results and related studies published by other authors we have noted that there is no a single case of a phase diagram with a *NAC* point which contains an interval of first-order *A*-*C* transitions [23]. This holds not only for concentration-temperature but for pressure-temperature diagrams as well [24]. Provided we have a small *A* range, this means that the proximity of the *I* phase to the *A* phase (which implies the absence or a small range of the existence for the *N* phase) is, in our opinion, another important factor influencing the character of the *A*-*C* transition. The effect of the *N* range can be included in a phenomenological model in an analogous fashion to that explaining the first-order nature of the *N*-*A* transition as the *N* range decreases [25], i.e., by adding the terms $-K\delta S\theta^2 + (\delta S)^2/2\chi$ to the free energy (2). Here $K > 0$ is

a coupling constant, δS represents the fluctuations of the nematic order-parameter, and χ is the susceptibility of these fluctuations. After minimizing respect to δS , the free energy is still given by (2) but a renormalized coefficient $b - \chi K^2/2$ is obtained for the fourth-order term. Clearly the proximity of the *I* phase to the *A* (and to the *C*) phase enhances the χ value and, therefore, favors the first-order condition for the *A-C* transition. If, as in our case, a broad *N* phase ($> 50^\circ\text{C}$) exists above the *A* phase, nematic fluctuations are negligible in comparison with those in compounds without an *N* phase and with a *C* phase close to the *I* phase. Thus, in spite of small *A* ranges and moderate polarizations we always obtain second-order *A-C** transitions.

In summary, we have presented experimental results of the temperature dependence of the spontaneous polarization and tilt angle in binary mixtures of two compounds

with *N-C** and *A-C** transitions, respectively. The behavior of these quantities indicates the existence of a tricritical point at or close to the *NAC** point. The analysis of ac calorimetric measurements corroborates this idea. Furthermore, in the light of the above results and by comparison with other similar studies, we conclude that, in order to obtain a first-order *A-C* transition, not only a narrow *A* range is necessary (wider for compounds with high P_s) but the proximity of the transition to the *I* phase is also required.

ACKNOWLEDGMENTS

This work is supported by the Comisión Interministerial de Ciencia y Tecnología of Spain (Projects Nos. MAT 91-0962-C02-02 and MAT 91-0923-C02-02).

-
- [1] Ch. Bahr and G. Heppke, *Mol. Cryst. Liq. Cryst.* **150b**, 313 (1987).
 - [2] B. R. Ratna, R. Shashidhar, G. G. Nair, S. K. Prasad, Ch. Bahr, and G. Heppke, *Phys. Rev. A* **37**, 1824 (1988).
 - [3] R. Shashidhar, B. R. Ratna, G. G. Nair, S. K. Prasad, Ch. Bahr, and G. Heppke, *Phys. Rev. Lett.* **61**, 547 (1988).
 - [4] D. Johnson, D. Allender, R. de Hoff, C. Maze, E. Oppenheim, and R. Reynolds, *Phys. Rev. B* **16**, 470 (1977).
 - [5] C. C. Huang and S. C. Lien, *Phys. Rev. Lett.* **47**, 1917 (1981).
 - [6] C. W. Garland and M. E. Huster, *Phys. Rev. A* **35**, 2365 (1987).
 - [7] X. Wen, C. W. Garland, and M. D. Wand, *Phys. Rev. A* **42**, 6087 (1991).
 - [8] C. C. Huang and S. C. Lien, *Phys. Rev. A* **31**, 2621 (1985).
 - [9] G. Heppke, D. Löttsch, and R. Shashidhar, *Liq. Cryst.* **5**, 489 (1989).
 - [10] H. Y. Liu, C. C. Huang, Ch. Bahr, and G. Heppke, *Phys. Rev. Lett.* **61**, 345 (1988).
 - [11] H. Y. Liu, C. C. Huang, T. Min, M. D. Wand, D. M. Walba, N. A. Clark, Ch. Bahr, and G. Heppke, *Phys. Rev. A* **40**, 6759 (1989).
 - [12] J. S. Patel, T. M. Leslie, and J. W. Goodby, *Ferroelectrics* **59**, 137 (1984).
 - [13] J. Etxebarria, A. Remón, M. J. Tello, A. Ezcurra, M. A. Pérez Jubindo, and M. T. Sierra, *Mol. Cryst. Liq. Cryst.* **150b**, 257 (1987).
 - [14] M. A. Pérez Jubindo, J. Fernández, and M. J. Tello, *J. Phys. D* **14**, 2305 (1981).
 - [15] K. Miyasato, S. Abe, H. Takezoe, A. Fukuda, and E. Kuze, *Jpn. J. Appl. Phys.* **22**, L661 (1983).
 - [16] C. W. Garland, *Thermochim. Acta* **88**, 127 (1985).
 - [17] J. A. Puértolas and M. Castro (unpublished).
 - [18] J. Boerio-Goates, C. W. Garland, and R. Shashidhar, *Phys. Rev. A* **41**, 3192 (1990).
 - [19] M. E. Huster, K. J. Stine, and C. W. Garland, *Phys. Rev. A* **36**, 2364 (1987).
 - [20] A. Rappaport and N. A. Clark (unpublished).
 - [21] C. W. Garland, G. Nounesis, K. J. Stine, and G. Heppke, *J. Phys. (Paris)* **50**, 2291 (1989).
 - [22] S. K. Prasad, V. N. Raja, D. S. Shankar Rao, G. G. Nair, and M. E. Neubert, *Phys. Rev. A* **42**, 2479 (1990).
 - [23] Preliminary results reported in D. A. Parmar, N. A. Clark, D. W. Walba, and M. D. Wand, *Phys. Rev. Lett.* **62**, 2136 (1989), presented an example of a phase diagram with a *NAC** point away from the tricritical point on the *A-C** line. However, subsequent high-resolution ac calorimetric studies carried out on the same system (Ref. [7]) did not confirm this point.
 - [24] C. Legrand, N. Isaert, J. Hmine, J. M. Buisine, J. P. Parneix, H. T. Nguyen, and C. Destrade, *J. Phys. II (France)* **2**, 1545 (1992).
 - [25] P. G. de Gennes, *The Physics of Liquid Crystals* (Clarendon, Oxford, 1974), pp. 316–318.